World Academy of Science, Engineering and Technology
International Journal of Mechanical and Mechatronics Engineering
Vol:5, No:1, 2011

Two Dimensional Simulation of Fluid Flow and Heat Transfer in the Transition Flow Regime using a Lattice Boltzmann Approach

Mehdi Shamshiri, Mahmud Ashrafizaadeh

***Abstract*—**The significant effects of the interactions between the system boundaries and the near wall molecules in miniaturized gaseous devices lead to the formation of the Knudsen layer in which the Navier-Stokes-Fourier (NSF) equations fail to predict the correct associated phenomena. In this paper, the well-known lattice Boltzmann method (LBM) is employed to simulate the fluid flow and heat transfer processes in rarefied gaseous micro media. Persuaded by the problematic deficiency of the LBM in capturing the Knudsen layer phenomena, present study tends to concentrate on the effective molecular mean free path concept the main essence of which is to compensate the incapability of this mesoscopic method in dealing with the momentum and energy transport within the above mentioned kinetic boundary layer. The results show qualitative and quantitative accuracy comparable to the solutions of the linearized Boltzmann equation or the DSMC data for the Knudsen numbers of $O(1)$.

***Keywords*—** Fluid flow and Heat transfer, Knudsen layer, Lattice Boltzmann method (LBM), Micro-scale numerical simulation, Transition regime.

I. Introduction

DUO to its indispensability of implementation in different scientific and industrial fields, the branch of the so-called micro-electro-mechanical systems (MEMS) has attracted much consideration in recent years [1]. Hence, a special understanding of the physics associated with the flow and heat transfer in miniaturized devices – which is completely different from that of their macroscale counterparts – seems to be absolutely necessary. Because of the larger surface to volume ratio of the micro-fluidic systems, the interactions of the fluid molecules with the solid walls may have significant influences on the macroscopic properties of the flow in this scale. Moreover, the dynamics of the above mentioned interactions differ substantially from macro scale [2].

As a micro-scale point of view, different flow regimes may be encountered as the mean free path of the molecules λ – the flight distance of the molecules before colliding into each other – becomes comparable with the characteristic length of the system H. In other words, the main attributes of the micro-scale flows can be characterized through a nondimensional number called Knudsen number which is defined as the ratio of the mean free path of the molecules to the characteristic length of the system $(Kn = \lambda / H)$. It should be noted that λ, itself, is related to the macroscopic quantities of the flow via $\lambda = (\mu / P)\sqrt{\pi k_B T / 2m}$ where μ is the viscosity, P is the pressure, m is the molecular mass, k_B is the Boltzmann's constant, and T is the absolute temperature.

The case of $Kn < 0.01$ is referred to as the continuum regime, in which the conventional hydrodynamic equations, i.e., the Navier-Stokes equations with no velocity slip boundary conditions and the Fourier heat conduction equation with no temperature jump boundary condition, are the appropriate governing equations. However as Kn increases to the limit of $0.01 \le Kn < 0.1$, which is treated as the slip flow regime, the already mentioned boundary conditions seem to fail and velocity slip and temperature jump will appear on the solid boundaries and the Navier-Stokes-Fourier (NSF) equations should be solved subject to the slip/jump boundary conditions. The values of $0.1 \le Kn < 10$ is related to the transition flow regime in which the continuum descriptions break down and consequently the NSF equations with velocity slip and temperature jump boundary conditions are also invalid. In order to predict the realistic characteristic of the flow in this regime, one may need to deal with the molecular based models such as direct simulation Monte-Carlo (DSMC), Boltzmann equation (BE) or molecular dynamics (MD). In the flow regime of $Kn \ge 10$, which is known as the free molecular flow regime, the transport process is assumed to be ballistic, since the rate of molecular interactions is much less than the rate of molecule-wall interactions [3]-[5].

Even though there have been much prosperous endeavors in simulating high speed transition flow problems using molecular based methods such as the direct simulation Monte Carlo (DSMC) and the direct solution of the Boltzmann equation (BE), the prospect of applying these methods to low-speed, low Knudsen number flows is frustrated due to high computational costs and special requirements to reduce large statistical scatter of the former and complexities associated with the solution of the nonlinear differential-integral equation of the latter [6], [7].

M. Shamshiri is a MSc. student of mechanical engineering at Isfahan University of Technology. Isfahan, 84156-8311, Iran (corresponding author; e-mail: m.shamshiri@me.iut.ac.ir).

M. Ashrafizaadeh is an assistant professor of mechanical engineering at Isfahan University of Technology and the head of university's High Performance Computing Center. Isfahan University of Technology, Isfahan, 84156-8311, Iran (e-mail: mahmud@cc.iut.ac.ir).

In the past two decades, a mesoscopic approach based on the evolution of the single-particle distribution function known as lattice Boltzmann method (LBM), has shown its potency to be considered as a powerful and promising numerical approach for simulating a wide range of flow and heat transfer problems including macro-, micro- and nano-fluidic applications [8]-[12]. The exceptional and peerless features of the LBM, e.g., having a kinetic nature, being a simplified solver of the Boltzmann equation (BE), explicitness of its dominant equation, simple programming procedure, easy boundary treatment and finally, intrinsic parallelism of its algorithm, have transmuted this method to a powerful and prevailing computational tool in challenging with complex fluid systems, e.g., porous media, multi phase and multi component flows [13]-[15]. In contrast with the MD method, in the LBM the computational effort is not related to the number of the fluid molecules. Instead, it depends on the number of the lattice nodes (or particles) and the lattice model (which demonstrates the lattice dimension and number of lattice links). Hence, LBM has emerged as a computationally efficient method, especially, for the case of micro- and nano-fluidic systems.

II. LATTICE BOLTZMANN METHOD

Following the work of He, Chen and Doolen [16] and Shi, Zhao and Guo [17], who recently proposed thermal lattice Boltzmann BGK models which employ two discrete evolution equations for density- and internal energy distribution function, i.e., f_k and g_k, respectively, the governing equations can be written as

$$f_k\left(x+e_k\delta t,t+\delta t\right)-f_k\left(x,t\right)=-\frac{1}{\tau}\left[f_k\left(x,t\right)-f_k^{eq}\left(x,t\right)\right]$$
$$g_k\left(x+e_k\delta t,t+\delta t\right)-g_k\left(x,t\right)=-\frac{1}{\tau_t}\left[g_k\left(x,t\right)-g_k^{eq}\left(x,t\right)\right] \quad (1)$$

where f_k^{eq} and g_k^{eq} are the density and energy distribution functions at equilibrium state, respectively, τ and τ_t are the relaxation times associated with the momentum and energy transport processes, dt is the time step and e_{ki} is the discrete velocity component along each lattice link. Note that because of the insignificant effects of the viscous heating in low-speed micro-scale gas flows, the term involving such effects has not been taken into account in our study and the simplest form of Shi's model [16] is applied.

Once the evolution process is done, the hydro and thermal macroscopic quantities (density, velocity and internal energy) can be then recovered from the following relations

$$\rho=\sum_{k=0}^{8}f_k$$
$$\rho u_i=\sum_{k=0}^{8}e_{ki}f_k \quad (2)$$
$$\rho\varepsilon=\sum_{k=0}^{8}g_k$$

where $\varepsilon=\frac{DRT}{2}$, D is the number of physical dimensions (here $D=2$) and R is the gas constant.

Using the two dimensional, nine-velocity lattice model $(D2Q9)$ illustrated in Fig. 1, the equilibrium distribution functions read

$$f_k^{eq}=\rho w_k\left[1+\frac{e_{ki}u_i}{c_s^{\,2}}+\frac{\left(e_{ki}u_i\right)^2}{2c_s^{\,4}}-\frac{u_iu_i}{2c_s^{\,2}}\right]$$
$$g_k^{eq}=\rho w_k\varepsilon\left[1+\frac{e_{ki}u_i}{c_s^{\,2}}+\frac{\left(e_{ki}u_i\right)^2}{2c_s^{\,4}}-\frac{u_iu_i}{2c_s^{\,2}}\right] \quad (3)$$

where c_s is the sound speed and w_k is the weight function for each lattice link given by

$$w_0=\frac{4}{9}\ ;\ w_k=\frac{1}{9}\quad k=1-4\ ;\ w_k=\frac{1}{36}\quad k=5-8 \quad (4)$$

and the discrete velocity components along D2Q9 lattice links e_k (k=0-8) can be denoted as

$$e_k=\begin{bmatrix}0&1&0&-1&0&1&-1&-1&1\\0&0&1&0&-1&1&1&-1&-1\end{bmatrix}c \quad (5)$$

here $c=\sqrt{3RT}$ is the r.m.s molecular speed which is equal to unity in this model. The sound speed is related to the r.m.s molecular speed through $c_s^{\,2}=C2/3$.

The pressure, kinematic viscosity and thermal diffusivity are obtained from $P=\rho c_s^{\,2}$, $\upsilon=\left(\tau-0.5\right)c_s^{\,2}\delta t$ and $\alpha=\left(\tau_t-0.5\right)c_s^{\,2}\delta t$, respectively. It's worth mentioning that one of the most important features of the above double distribution function lattice Boltzmann model is that the Prandtl number $\Pr=\left(\tau-0.5\right)/\left(\tau_t-0.5\right)$ is no longer fixed as a constant.

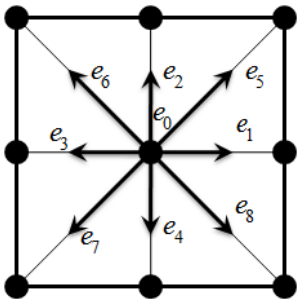

Fig. 1 Lattice links for the D2Q9 lattice Boltzmann model

III. KNUDSEN LAYER, BOUNDARY CONDITIONS, RELAXATION TIME AND EFFECTIVE MEAN FREE PATH CONCEPTS

The major challenges in dealing with micro-scale modeling through LBM are the application of the correct boundary conditions in order to capture the real velocity slip and temperature jump at the boundaries and the establishment of a proper relation between the Knudsen number and the relaxation time of the method. Hence, in the proceeding sub-sections, the issues of the kinetic boundary conditions and the Kn-dependent relaxation time will be discussed and correspondingly, the concept of the Knudsen layer and effective mean free path will be addressed.

A. Knudsen layer

The significant effects of the interactions between the system walls and the gas molecules constitute a kinetic boundary layer with a thickness of $\mathrm{O}(\lambda)$ at the vicinity of the solid walls, known as Knudsen layer. In this layer the conventional NSF equations are incapable of predicting the realistic phenomena associated with the momentum- and energy transport and especial solutions of the continuous Boltzmann equation (CBE) are required for this purpose. The reason must be sought in the breakdown of the linear constitutive relations defining the stress tensor and the heat flux vector in this layer. Consequently, according to the occurrence of a finite slip, there would be a significant difference between the wall velocity and temperature (u_w, T_w) and the velocity and temperature of the gas located at the vicinity of the wall (u_s, T_s) which leads to the following nondimensional slip/jump boundary conditions [4]

$$U_s - U_w = \frac{2-\sigma_v}{\sigma_v}\left[Kn\left(\frac{\partial U}{\partial n}\right)_s + \frac{Kn^2}{2}\left(\frac{\partial^2 U}{\partial n^2}\right)_s \right] \tag{6}$$

$$T_s - T_w = \frac{2-\sigma_T}{\sigma_T}\left[\frac{2\gamma}{\gamma+1}\right]\frac{1}{\mathrm{Pr}}\left[Kn\left(\frac{\partial T}{\partial n}\right)_s + \frac{Kn^2}{2}\left(\frac{\partial^2 T}{\partial n^2}\right)_s \right]$$

where n stands for the normal (unit) coordinate to the wall, γ is the ratio of specific heats, σ_v and σ_T are the momentum and energy accommodation coefficients, respectively, Kn is the Knudsen number, and finally, Pr is the Prandtl number which is defined as $\mathrm{Pr} = \frac{c_p \mu}{k}$ (here c_p is the specific heat at constant pressure and k is the thermal conductivity coefficient). The details of these models and their associated concepts are widely available in the literature, e.g, [4].

B. Boundary conditions

In order to model the velocity slip at the boundary, the Maxwellian kinetic boundary condition with the assumption of a fully diffuse molecular reflection has been employed to determine the unknown distribution functions at the boundary coming to the flow domain from outside of the solid wall which reads [18], [19]

$$f_k(x, t+\delta t) = \frac{\sum_{(e_{k'}-u_w).n<0} \left|(e_{k'}-u_w).n\right| f_{k'}(x, t+\delta t)}{\sum_{(e_{k'}-u_w).n>0} \left|(e_k-u_w).n\right| f_k^{eq}(x, \rho_w, u_w)} \times f_k^{eq}(x, \rho_w, u_w) \tag{7}$$

where k and k' refer to the directions of the reflected and incoming lattice particles, u_w and ρ_w are the velocity and density at the wall, respectively, and n is the inward unit normal vector of the solid boundary. More clearly, in the above expression, the k-ward distribution functions f_k on the walls are unknown (shown with dashed arrows in Fig. 2) and need to be determined using the known k'-ward distribution functions $f_{k'}$ (shown with solid arrows in the same figure) according to the already mentioned Maxwellian rule.

In order to capture the temperature jump at the wall, the unknown k-ward energy distribution functions, should be defined. For this objective, one may obey the spirit of the Maxwellian diffuse reflection which states that the reflected molecules are in thermal equilibrium with the solid boundary. With respect to this idea, we have [20]

$$g_k = \frac{DRT_w}{2} f_k \tag{8}$$

where T_w is the temperature of the wall. A similar set of diffuse scattering boundary conditions for thermal flows has been proposed by Niu, Shu and Chew [21], which is based on the assumption that the incoming particles toward the wall forget their previous information and reemit so that they satisfy the mass-balance and normal-flux conditions and is shown to be equivalent to the second order boundary conditions in (6).

C. Relaxation time

In a two-dimensional nine-velocity lattice BGK model (D2Q9) the Knudsen number can be written in terms of the relaxation time as [10]

$$Kn = \sqrt{\frac{8}{3\pi}}\frac{(\tau - 0.5)}{N_H} \tag{9}$$

where N_H is the number of lattice sites across the channel height H, i.e., $N_H = H/\delta x$ (δx is the lattice length).

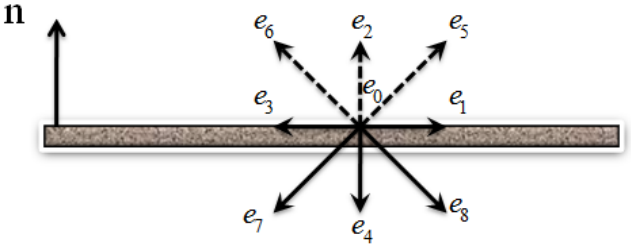

Fig. 2 Schematic diagram of the known (solid arrows) and unknown (dashed arrows) distribution functions for the bottom wall

D.Effective mean free path

Many authors – in individual issues – have reported the prosperity of the LBM in going beyond the NSF equations and simulating the flow and heat transfer in the slip and transition flow regimes [21]-[25]. In contrast, recent studies have denoted that the current LB models are unable to capture the correct flow properties, especially in the near-wall region [20], [26]-[28]. Figs. 3 and 4 are schematic diagrams of the considerable difference between the real velocity and temperature profiles and those obtained from the NSF equations and common LB models for some typical rarefied shear-driven and Fourier flows which state that the already mentioned methods are unable to capture the realistic macro properties of such micro-scale problem. Moreover, it is observed that the difference between the predictions of such methods and the actual quantities increases as the wall is approached and vanishes at the vicinity of the core region.

Regarding this problematic deficiency of the LBM, some possible strategies were proposed in order to enable the capturing of the Knudsen layer phenomena within the framework of this mesoscopic method. Recently, Zhang, Gu, Barber and Emerson [20], [27] introduced the concept of the spatio-variational mean free path. The main idea behind this procedure is that the solid surface affects the near-wall region through causing substantial reduction in the mean time between consecutive collisions of the gas molecules located close to the wall compared to that of the bulk flow molecules. Consequently, there would be a significant reduction in the average distance that near-wall gas molecules travel before colliding each other, i.e., the mean free path λ. This promising procedure – which is employed in our study – is briefly outlined in the following. The effective mean free path λ_{eff} that accounts for the reduction of λ in the near-wall region can be expressed as

$$\begin{cases} \lambda_{eff} = \dfrac{\lambda}{1+\psi\left(y/\lambda\right)} \\ \psi\left(y/\lambda\right) = 0.7\exp\left(-c\dfrac{y}{\lambda}\right) \end{cases} \tag{10}$$

here y is the distance normal to the solid wall, λ is the mean free path, c is a constant through which the extent of the Knudsen layer can be controlled and depends on the governing equations. In the current work we set $c=1$.

For non isothermal flows, the influence of density and temperature on the mean free path should be considered, which leads to the following relation for the λ_{eff}

$$\frac{\lambda_{eff}}{\lambda_{ref}} = \frac{1}{1+\psi\left(y/\lambda\right)}\frac{\rho_{ref}}{\rho}\left(\frac{T}{T_{ref}}\right)^{\omega-0.5} \tag{11}$$

here λ_{ref} and ρ_{ref} are the mean free path and density at a reference temperature, say T_{ref}, local macroscopic density and temperature are denoted by ρ and T, respectively, and finally ω is a parameter which depends on the employed molecular interaction model taking a value of 0 for hard-sphere molecular interactions and 1 for Maxwellian interactions.

Considering how temperature affects the mean free path of the molecules and substituting its corresponding expression in (9), allows the local relaxation time to be formulated as [29]

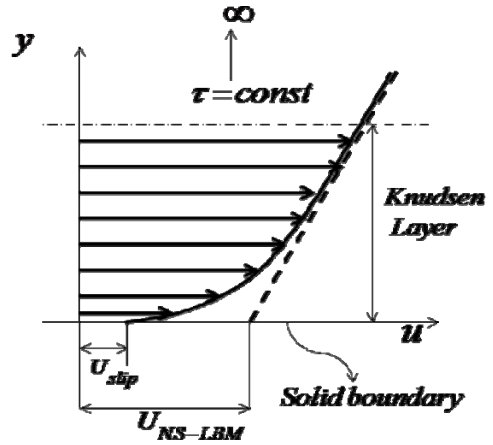

Fig. 3 Schematic diagram showing velocity defect in the Knudsen layer for a rarefied gaseous shear driven flow, where U_{slip} and U_{NS-LBM} represent the microscopic and macroscopic velocity slip, respectively. Real velocity profile predicted by kinetic theory (——) and profile obtained from NS equations and common LB models (– – –).

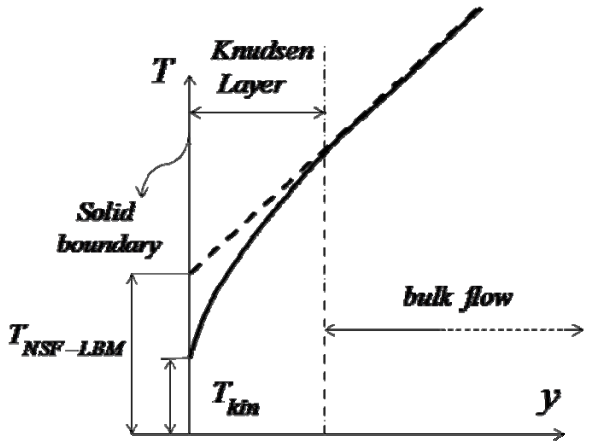

Fig. 4 Schematic diagram showing Temperature over-prediction in the Knudsen layer for a rarefied gaseous Fourier flow, where T_{kin} and $T_{NSF-LBM}$ represent the microscopic- and macroscopic Temperature jump, respectively. Actual Temperature profile predicted by kinetic theory (——) and profile obtained from *NSF* equations and common LB models (– – –).

$$\tau = \sqrt{\frac{3\pi}{8}}\left(\frac{KnN_H}{1+\psi(y/\lambda)}\right)\frac{\rho_{ref}}{\rho}\left(\frac{T}{T_{ref}}\right)^{\omega-0.5} + 0.5 \quad (12)$$

where $Kn = \lambda_{ref}/H$. Finally, the thermal relaxation time can be obtained via $\tau_t = (\tau - 0.5)/\Pr + 0.5$.

It should be bore in mind that the above correction factor is developed for the isothermal Kramers' problem – which is a gas bounded by a planner surface and under a constant shear stress – in which the overlap of the Knudsen layers is not encountered. In contrast with the Kramers' problem, in the case of the channel flow the Knudsen layers attached to the solid walls start to overlap by the increase in the Knudsen number and this should be taken into account through another correction function which is given by

$$\varphi(y/\lambda) = \psi(y/\lambda) + \psi\left[(H-y)/\lambda\right] \quad (13)$$

where H is the height of the channel, y is the distance from one of the walls while $H - y$ is the distance from the other one. Summarily, all the previous relations for the Kramers' problem can correspondingly be applied to the channel flow if ψ is replaced by φ.

IV. Results and Discussions

To demonstrate advantages of implementing the wall function concept in the LBM, some typical cases of the shear-driven and thermal rarefied flows, namely, the planner Couette and Fourier flows confined between two parallel plates for a range of Knudsen numbers are simulated in this section and the results are validated using those of the solutions of the linearized Boltzmann equation given by Sone, Takata and Ohwada [30] for the Couette flow and the DSMC data obtained by Gallis, Rader and Torczynski [31] for the rarefied Fourier flow. Hereafter we adopt a rescaled Knudsen number $K\left(=\sqrt{\pi/2}\,Kn\right)$ as a new parameter to match our results with [30].

A. Planner Couette flow

The first case study is a planner Couette flow confined between two plates (walls) parallel to the x-axis separated by distance H, which are moving oppositely with a constant velocity $\pm U_w$. The kinetic boundary condition of (7) is used to describe the gas surface interactions with the solid walls after the streaming process of the particles, while periodic boundary conditions are employed at the inlet and outlet.

Figs. 5 and 6 show the grid-independent normalized velocity U/U_w profiles versus the nondimensional distance y/H at different degrees of the rarefaction. At low values of K the effect of the Knudsen layer on the flow domain is minimal and as a consequence, for $K = 0.001$, namely in the continuum regime, the predicted velocity profiles with and without the local mean free path correction are almost identical (Fig. 5).

Fig. 6 illustrates the velocity profiles of the planner Couette flow in the early transition flow regime, namely, at $K = 0.1 - 1.0$, respectively. The results are compared with the solutions of the linearized Boltzmann equation [30]. As shown in this figure, the magnitude of the velocity slips on the plates increase as K becomes larger since the extent of the Knudsen layers attached to the walls become larger and larger. Furthermore, one can observe from this figure that the main characteristics of the rarefaction effects, i.e., the nonlinear velocity profile in the Knudsen layer and the overlap effects of the Knudsen layers at the upper and lower walls are well captured in the present simulation and the predicted results are in relatively good agreement with those given by [30] both in the near-wall- and core regions up to the the rescaled Knudsen numbers of $\mathrm{O}(1)$.

B. Rarefied Fourier flow

As the second case study we consider a planner rarefied Fourier flow confined between two plates parallel to the x-axis at $y = \pm H/2$. Both of the plates (walls) are assumed to be stationary and are kept at constant temperatures $T_C = 263K$ (lower plate) and $T_H = 283K$ (upper plate), respectively. The simulations are carried out using an argon-like monatomic gas with a Maxwellian collision model which coerces the viscosity temperature exponent ω to be equal to unity ($\omega = 1$). The Prandtl number is fixed at 0.67 and the reference temperature is considered as $T_{ref} = (T_H + T_L)/2 = 273K$. All other parameters are set to those used by [31] for consistency with the DSMC data.

The initial conditions for flow and temperature fields are a zero velocity distribution and a constant temperature profile T_{ref}, respectively. The Maxwellian diffuse scattering boundary conditions of (7) and (8) are used to describe the molecular interactions with the solid walls after the streaming process of the particles, while periodic boundary conditions are employed at the inlet and outlet.

Figs. 7 and 8 show the grid-independent normalized temperature $\left[\frac{T(y)-T_C}{T_H-T_C}\right]$ profiles as a function of the nondimensional distance y/H for the already mentioned case study, at different degrees of the rarefaction. To validate the present approach, the DSMC data given by [31] is also included. Again, at low Knudsen numbers, i.e., the continuum limit, the Knudsen layer correction doesn't play a significant role on the mean free path – which emanates from the negligible effects of the Knudsen layer in this flow regime – and hence the differences between the results of the simulation with and without this modification

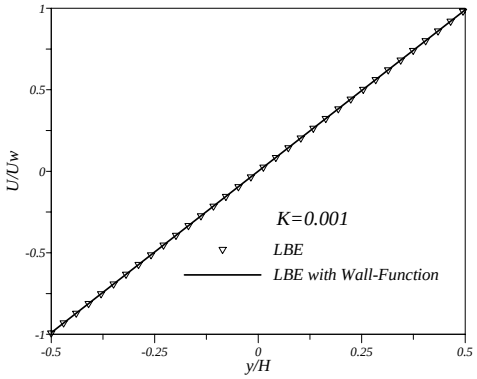

Fig. 5 Normalized velocity profile for shear driven Couette flow in the continuum limit.

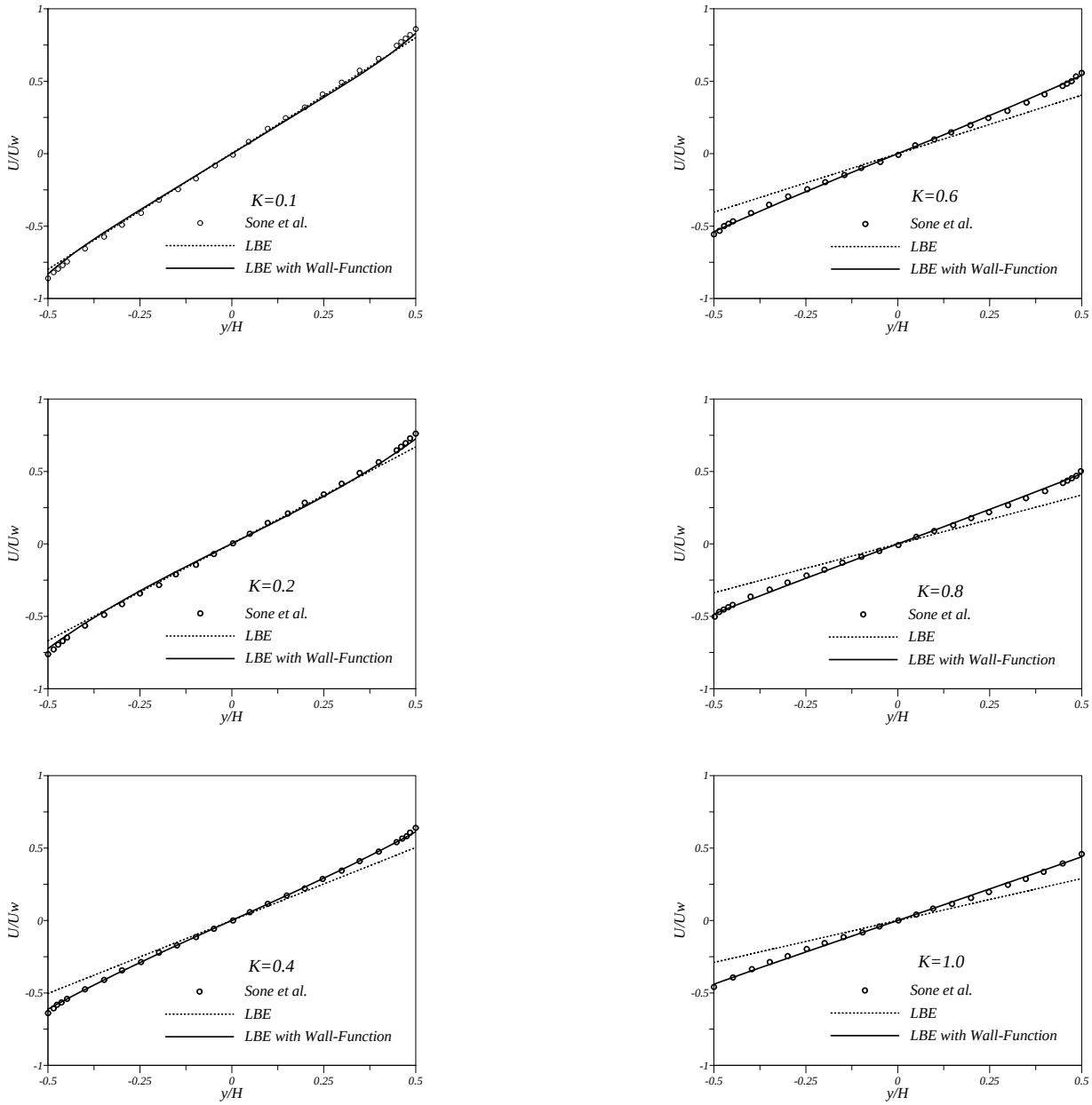

Fig. 6 The Normalized velocity profiles for rarefied shear driven Couette flow in the transition regime. Our LB results are compared with the data given by [30].

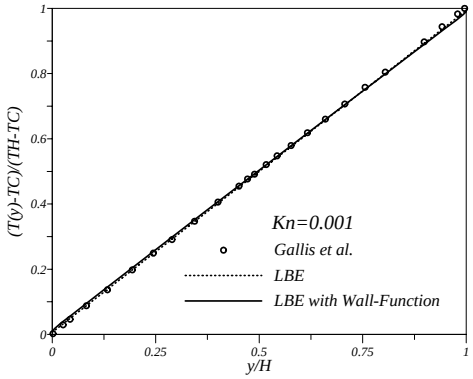

Fig. 7 Normalized temperature profiles for rarefied Fourier flow in the continuum flow regime.

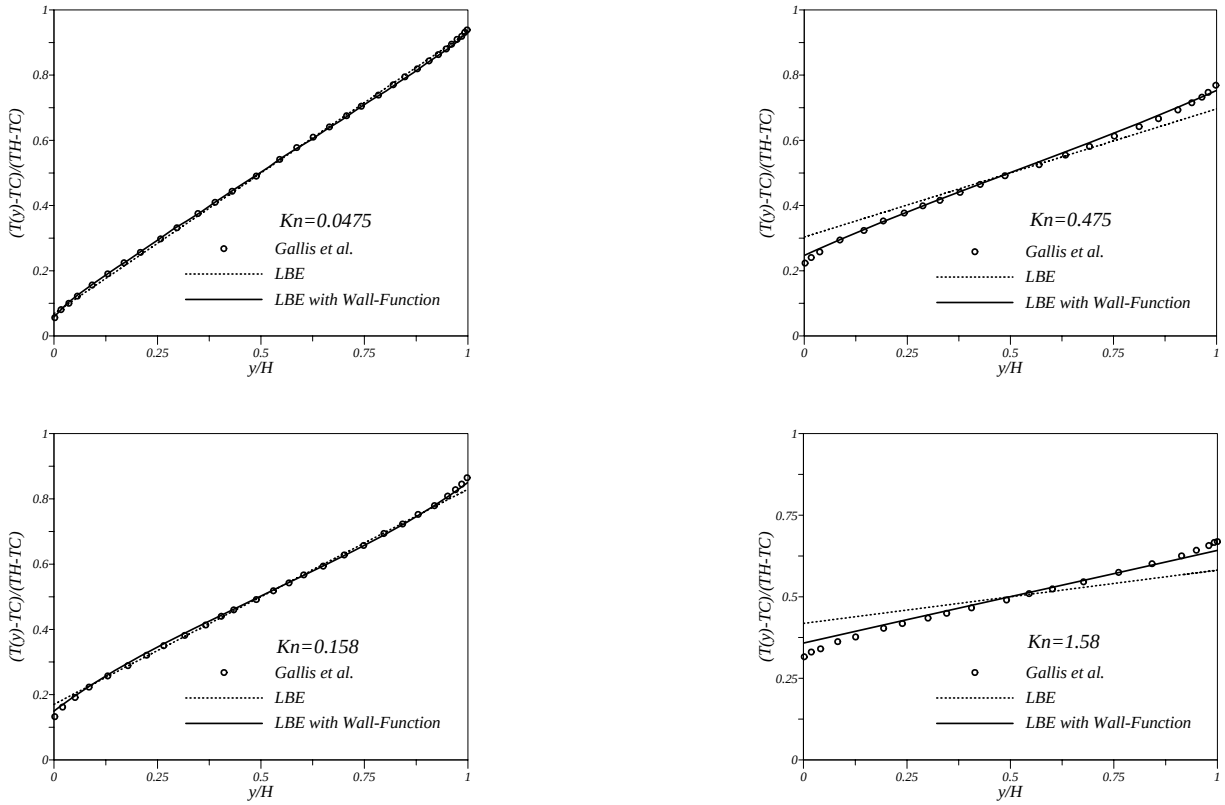

Fig. 8 The normalized temperature profiles of the rarefied Fourier flow in the transition flow regime. Our LB results are compared with the DSMC data given by [31].

and the DSMC data can be hardly distinguished which is shown for $Kn = 0.001$ (Fig. 7). But as the Knudsen number approaches higher values, namely, the transition flow regime, the results of the standard LBE departs further from those of the DSMC data and as can be seen, the predicted profiles of this non-modified model proffer a linear temperament for temperature variation across the channel that is inconsistent with the nonlinear physical inclination of the actual temperature profiles within the Knudsen layer (Fig. 8). However, implementation of the wall function technique enables the capturing of both the nonlinear temperature variation in the near-wall region and the overlap effects of the Knudsen layers at the upper and lower walls – that are the direct nonequilibrium effects of the rarefaction phenomenon – and results in satisfactory heat transfer predictions comparable with the DSMC data even at a relatively moderate transitional Knudsen number suchlike $Kn = 1.58$. In addition, it can be concluded from the plots that an increase in the Knudsen number leads to the flatter temperature profiles which is the obvious consequent of the increasing temperature jump at the channel walls.

V. CONCLUSIONS

In summary, a geometry dependent wall function technique has been implemented in the standard lattice Boltzmann BGK model in order to rectify the inadequacies associated with this mesoscopic method in dealing with the momentum and energy transport within the Knudsen layer and to enhance the potency

of such a numerical method in challenging with the simulation of the micro-scale rarefied gaseous flows. The procedure has been successfully applied to some typical rarefied shear-driven and Fourier flows between two parallel plates and the results are shown to be in relatively excellent agreement with those of the linearized Boltzmann equation and the DSMC data ,respectively, for the Knudsen numbers of $O(1)$. In conclusion, the above mentioned technique seems to be promising and reliable for flow and heat transfer simulation of the miniaturized devices in the framework of the LBM.

REFERENCES

[1] C. M. Ho and Y. C. Tai, "Micro-electro-mechanical systems (MEMS) and fluid flows," in *Ann. Rev. Fluid Mech*. 30, p. 579, 1998.
[2] S. Roy, S. Chakraborty, "Near-wall effects in micro scale Couette flow and heat transfer in the Maxwell-slip regimes," in *Microfluid Nanofluid*, 3, 437–449, 2007.
[3] J. Chun and D. L. Koch, "A direct simulation Monte Carlo method for rarefied gas flows in the limit of small Mach number," *Phys. Fluids*, 17, 107107, 2005.
[4] G. E. Karniadakis, A. Beskok, and N. Aluru, *Micro flows and nano flows: Fundamentals and simulation*, Springer, New York, 2005.
[5] C. Cercignani, *Slow rarefied flows: Theory and application to Micro-electro-mechanical systems*, Birkhäuser Verlag, Basel, Switzerland, 2006.
[6] N. G. Hadjiconstantinou, A. Garcia, M. Bazant and G. He, "Statistical error in particle simulations of hydrodynamic phenomena," in *J. Comput. Phys*., 187, 274, 2003.
[7] F. Sharipov, L. M. G. Cumin, and D. Kalempa, "Plane Couette flow of binary gaseous mixture in the whole range of the Knudsen number," in *Eur. J. Mech. B/Fluids*, 23, 899, 2004.
[8] S. Chen and G. D. Doolen, "Lattice Boltzmann method for fluid flows," in *Ann Rev Fluid Mech*, 30:329-64, 1998.
[9] X. Nie, G. D. Doolen and S. Chen, "Lattice Boltzmann simulations of fluid flows in MEMS," in *J Stat Phys*, 107, (1/2), 279, 2002.
[10] Y. H. Zhang, R. S. Qin, Y. H. Sun, R. W. Barber, and D. R. Emerson, "Gas flow in microchannels – A lattice Boltzmann method approach," in *J. Stat. Phys.* 121, 257, 2005.
[11] W. S. Jiaung and J. R. Ho, "Lattice Boltzmann study on size effect with geometrical bending on phonon heat conduction in a nanoduct," in *J Appli. Physics*, V. 95, N. 3, 2004.
[12] D. Yua, R. Meia, L. S. Luo and W. Shyy, "Viscous flow computations with the method of lattice Boltzmann equation," in *Progress in Aerospace Sciences*, 39, 329–367, 2003.
[13] N. S. Martys and H. D. Chen, "Simulation of multicomponent fluids in complex three-dimensional geometries by the lattice Boltzmann method," in *Phys. Rev. E*, 53, 743, 1996.
[14] P. Zhou and C.W. Wu, "Numerical simulation of electrocapillary driven flows," in *Micro and Nanosystems*, 1, 57-62, 2009.
[15] Z. L. Guo and T. S. Zhao, "Discrete velocity and lattice Boltzmann models for binary mixtures of nonideal fluids," in *Phys. Rev. E*, 68, 035302(R), 2003.
[16] X. He, S. Chen and G. D. Doolen, "A novel thermal model for the lattice Boltzmann method in incompressible limit," in *J. Comput. Phys.*, 146, 282, 1998.
[17] Y. Shi, T. S. Zhao and Z. L. Guo, "Thermal lattice Bhatnagar-Gross-Krook model for flows with viscous heat dissipation in the incompressible limit," in *Phys. Rev. E*, 70, 066310, 2004.
[18] G. H. Tang, X. J. Gu, R. W. Barber, and D. R. Emerson, "Lattice Boltzmann simulation of nonequilibrium effects in oscillatory gas flow," in *Phys. Rev. E*, 78, 026706, 2008.
[19] Ansumali S. and Karlin I. V., "Kinetic boundary conditions in the lattice Boltzmann method," in *Phys. Rev. E*, 66, 026311, 2002.
[20] Y. H. Zhang, X. J. Gu, R. W. Barber and D. R. Emerson, "A thermal lattice Boltzmann model for low speed rarefied gas flow," Daresbury Laboratory Technical Report, TR- 2006-002, 2006.
[21] X.D. Niu, C. Shu and Y.T. Chew, "A thermal lattice Boltzmann model with diffuse scattering boundary condition for micro thermal flows," in *Computers & Fluids*, 36, 273–281, 2007.
[22] L. Zheng, B. C. Shi and Z. H. Chai, "Lattice Boltzmann method for simulating the temperature jump and velocity slip in microchannels," in *Commun. Comput. Phys*., Vol. 2, No. 6, 1125-1138, 2007.
[23] T. Lee and C. L. Lin, "Rarefaction and compressibility effects of the lattice-Boltzmann-equation method in a gas microchannel," in *Phys. Rev. E*, 71, 046706, 2005.
[24] Y. H. Zhang, R. S. Qin and D. R. Emerson, "Lattice Boltzmann simulation of rarefied gas flows in microchannels," in *Phys. Rev. E*, 71, 047702, 2005.
[25] H. P. Kavehpour, M. Faghri and Y. Asako, "Effects of compressibility and rarefaction on gaseous flows in microchannels," in *Numer Heat Transfer*, Part A: Applications, 32, 677 – 696, 1997.
[26] G. H. Tang, Y. H. Zhang and D. R. Emerson, "Lattice Boltzmann models for nonequilibrium gas flows," in *Phys. Rev. E*, 77, 046701, 2008.
[27] Y. H. Zhang, X. J. Gu, R. W. Barber and D. R. Emerson, "Capturing Knudsen layer phenomena using a lattice Boltzmann model," in *Phys. Rev. E*, 74, 046704, 2006.
[28] M. Ashrafizaadeh, and M. Shamshiri, "Two dimensional simulation of fluid flow in the Knudsen layer using a lattice Boltzmann approach," in *Proc. 13 Annual and 2nd international Fluid Dynamics Conference*, University of Shiraz, Shiraz, 2010, submitted for publication.
[29] G. H. Tang, Y. H. Zhang, X. J. Gu, R. W. Barber, and D. R. Emerson, "Lattice Boltzmann model for thermal transpiration," in *Phys. Rev. E*, 79, 027701, 2009.
[30] Y. Sone, S. Takata and T. Ohwada, "Numerical analysis of the plane Couette flow of a rarefied gas on the basis of the linearized Boltzmann equation for hard-sphere molecules," in *Eur. J. Mech. B-Fluids*, 9, 273, 1990.
[31] M. A. Gallis, D. J. Rader and J. R. Torczynski, "Calculations of the near-wall thermophoretic force in rarefied gas flow," in *Phys. Fluids*, 14, 4290, 2002.